Minimization of Critical Flow Velocity of Aeroelastic Energy Harvester via Delayed Feedback Control

Filip SARBINOWSKI, Roman STAROSTA

Poznan University of Technology, Institute of Applied Mechanics,
Jana Pawła II 24,60-965 Poznań, Poland
filip.j.sarbinowski@doctorate.put.poznan.pl
Poland,roman.starosta@put.poznan.pl

Abstract

The paper describes the procedure of modelling and optimization of the aeroelastic energy harvester from the point of view of their operation at very low flow velocities. Using analytical solutions of models of different device variants, the relationships between their efficiency and flow velocity were presented. By way of analytical considerations, the conditions for high performance operation of the device have been demonstrated, indicating at the same time the difficulty in maintaining it at low operation velocities. As a solution to the problem, the application of external delayed feedback control was proposed and its effectiveness was demonstrated.

Keywords: energy harvesting, delayed feedback control, flow induced vibrations

1. Introduction

The essence of aeroelastic energy harvesting is to convert mechanical energy of vibrations caused by flow on electrical energy. One of mechanisms of vibration excitation induced by constant flow is galloping – phenomena caused by occurrence of negative aerodynamic damping in the system. Mathematical model of this effect was first derived by Den Hartog in [1] and in the following years significantly extended i.a. in [2]. According to these works, we consider a body with one degree of freedom (translation parallel to axis Z), mounted on a damped spring system, subjected to flow in a direction parallel to the X axis (see Fig. 1). The dynamics of the system is described by the equation:

$$m\,\ddot{z}(\bar{t}) + c\,\dot{z}(\bar{t}) + s\big(z(\bar{t})\big) = F_z(\alpha) = \frac{1}{2}\,h\,\overline{\rho}\,U^2\,C_z(\alpha) \tag{1}$$

where: m – mass of the body [kg], c – damping coefficient [kg/s], $s(x(\bar{t}))$ – restoring force [N], $z(\bar{t})$ – displacement in Z direction [m], $\dot{()}$ and $\ddot{()}$ – first and second differential with respect to time, $C_z(\alpha)$ – coefficient of aerodynamic force acting in the Z direction for $\alpha = \dot{z}/U$ [-], F_Z – aerodynamic force component acting in the Z direction [N], h – characteristic length of the body [m], $\overline{\rho}$ – fluid density [kg/m^2], U – flow velocity [m/s].

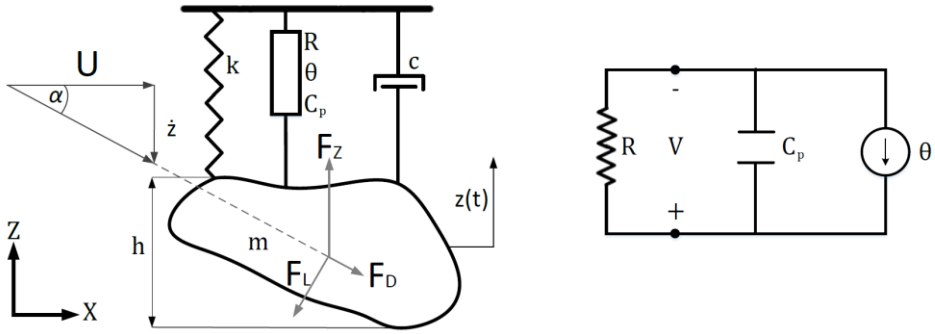

Figure 1. Physical model of aeroelastic energy harvester.
F_L – lift force, F_D – drag force

As reported in [3] and [4] the approximation of the $C_z(\alpha)$ function with a third order polynomial is sufficient for energy harvesting purposes. In addition, we assume that the flowed body has a symmetry axis in the direction normal to the flow. In this case, the even coefficients a_n will equal to zero:

$$\begin{cases} C_z(\alpha) = a_1\,\alpha + a_3\,\alpha^3 + \mathcal{O}(\alpha^4) \\ a_1 = \left(\dfrac{dC_L}{d\alpha} + C_D\right) \\ a_3 = \dfrac{1}{6}\left(\dfrac{d^3C_L}{d\alpha^3} + 3\dfrac{d^2C_D}{d\alpha^2}\right) \end{cases} \tag{2}$$

Conversion of mechanical energy into electricity can be carried out using a variety of transducers, however, the most commonly used are electrostatic, electromagnetic and piezoelectric. Electrostatic may be the cheapest solution for large scale production [5], [6]. Electromagnetic [7], [8], due to their complicated construction turn out to be the most expensive but at the same time characterized by high efficiency. The multitude of possible transducer designs of this type increases their versatility, allowing their use in both small devices [9] and massive hydro or wind power plants. Prototypes, however, most often are consist of piezoelectric transducers [10] – [12], which is justified by great simplicity in their implementation while maintaining high efficiency. It will also be used in this work. Due to the fact that the value of structural damping does not have a qualitative impact on the issue under consideration, it will be neglected ($c = 0$). Thus, the mathematical model of piezoelectric vibration energy harvester (PVEH) takes the form [13]:

$$\begin{cases} m\,\ddot{z}(\bar{t}) + s\big(z(\bar{t})\big) + \theta\,v(\bar{t}) = \dfrac{1}{2}\overline{\rho}U^2h\left(a_1\,\dfrac{\dot{z}(\bar{t})}{U} + a_3\left(\dfrac{\dot{z}(\bar{t})}{U}\right)^3\right) \\ Cp\,\dot{v}(t) + \dfrac{v(\bar{t})}{R} - \theta\,\dot{z}(\bar{t}) = 0 \end{cases} \tag{3}$$

where: *v(t)* – generated voltage [V], θ – electromechanical coupling [N/V], R – circuit resistance [Ω], Cp – circuit equivalent capacity [F]. Mathematical model (eq. 3) can rewritten in dimensionless form by introducing dimensionless parameters:

$$\begin{cases} \ddot{x}(t) + S(x(t)) + \kappa\, n(\tau) = a_1\, \rho\, u\, \dot{x}(t) + a_3\, \rho \dfrac{\dot{x}(t)^3}{u^3} \\ \dot{n}(\tau) + \dfrac{n(t)}{r} - \dot{x}(t) = 0 \end{cases} \tag{4}$$

where: $x(t) = \frac{z(t)}{h}$, $n(t) = \frac{v(t)}{\theta\, Cp} h$, $\kappa = \frac{\theta^2}{Cp\, m\, {\omega_n}^2}$, $\rho = \frac{h^2\, \bar{\rho}}{2m}$, $r = Cp\, \omega_n\, R$, $u = \frac{U}{h\, \omega_n}$, $t = \omega_n\, \bar{t}$ and $S(x(t))$ – dimensionless restoring force.

The efficiency of the device is largely determinated by the geometry of the flowing body, which in the model (eq. 3) is represented by coefficients a_1 and a_3. In [14], elliptical cross-sections with different ratios between the length of the semi-minor axis and the semi-major axis were examined. A substantial set of aerodynamic coefficients of various typical sections is included in [15]. The maximum efficiency of PVEH depending on the shape of the flowing body was analyzed in [16].

Another factor strongly affecting the performance of PVEH is its mechanical structure. The typical one degree of freedom beam devices ([17], [18], [19]) seem to give way in this respect to more complex systems with many degrees of freedom [20]). It is worth noting that devices showing also torsional vibrations should not be modeled using the Den Hartog's hypothesis – for torsional vibrations the quasi-stationarity condition is never satisfied. The nonstationary flow model was used, among others in work [21]. One can also indicate many variants of the device with nonlinear mechanical properties [22], but – according to the best knowledge of the authors – no work has been done so far to compare and evaluate them.

2. Efficiency study

The energy generated by the device depends on the flow velocity to which it is exposed. In order to determine this relationship, the mathematical model of the device (eq. 3) will be solved by utilizing the Harmonic Balance Method, adopting first a linear model of restoring force $S(x) = k\, x(t)$. Analyzing the numerical solutions of the system and assuming initial velocity of the system $\dot{x}(t) = 0$ it was determined that it would be sufficient to set up solutions in the form:

$$x(t) = A_x \cos(\omega t) \tag{5}$$

$$n(t) = A_N \cos(\omega t + \varphi) \tag{6}$$

where: A_x – dimensionless amplitude of vibration, A_N – dimensionelss voltage amplitude, ω – dimensionless frequency and φ – phase shift are unknown quantities. Substituting the assumed solutions (eq**.** 5-6) into the governing equations (4) and then balancing the harmonics in both equations, we obtain a system of equations, that – with bypassing trivial solutions – leads to obtaining the following identities:

$$\begin{cases} \sin(\varphi) = \dfrac{1}{\sqrt{(r\omega)^2+1}} \\ \cos(\varphi) = \dfrac{r\omega}{\sqrt{(r\omega)^2+1}} \\ A_N = A_x \dfrac{r\omega}{\sqrt{1+r^2\omega^2}} \\ \omega = \sqrt{\dfrac{kr^2+r^2\kappa-1+\sqrt{4kr^2+(kr^2+r^2\kappa-1)^2}}{2r^2}} \\ A_x = \sqrt{\dfrac{4u(r\kappa-a_1u\rho(1+r^2\omega^2)}{3a_3\rho\omega^2(1+r^2\omega^2)}} \end{cases} \tag{7}$$

The average electrical power is defined as:

$$P = \frac{1}{T}\int_0^T \frac{n(t)^2}{r}dt = \frac{{A_N}^2}{2r} \tag{8}$$

where $T = \frac{2\pi}{\omega}$ stands for vibration period. By referring power P to the total flow power $P_t = u^3\rho$ together with the application of identities (eq. 7) allows the formal definition of device efficiency η as a function of flow velocity:

$$\eta = \frac{P}{P_t} = \frac{2r\kappa(a_1u\rho(1+r^2\omega^2)-r\kappa)}{3a_3u^2\rho^2(1+r^2\omega^2)^2} \tag{9}$$

Figure 2 represents the function (9) for various system parameters. On each of the curves, three values can be observed: critical velocity u_{cr} such that $\eta(u_{cr}) = 0$, resonance velocity u_R, for which $\frac{\partial\eta}{\partial u} = 0$ and peak efficiency $\eta(u_R) = -\frac{{a_1}^2}{6a_3}$.

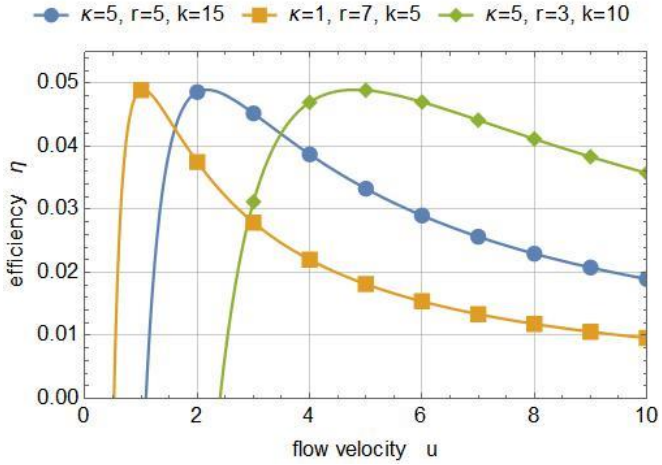

Figure 2. Efficiency vs flow velocity for different sets of parameters

It should be noted that as the critical velocity u_R of the system decreases, its operating range at high efficiency significantly narrows, thus the device designed for recovering energy from slow flows would only work effectively in a very narrow velocity band and even a slight deviation from the assumed operation conditions would cause a dramatic decrease in the efficiency of the device.

Reduction in this negative effect can be sought in the features of the device with nonlinear restoring force model in form of $S(x) = k\,x(t) + k_N\,x(t)^3$. Since the modification of the stiffness does not affect the second equation of the model (eq. 3), the expressions for the phase shift φ and the relationship between the vibration amplitude and the voltage remain unchanged, while the system of equations that allows to determine the frequency of the vibrations ω and the amplitude of the vibrations A_x takes the form:

$$\begin{cases} \omega^2 - k - \dfrac{r^2\kappa\omega^2}{1+r^2\omega^2} - \dfrac{3k_N A_x^2}{4} = 0 \\ \dfrac{r\kappa}{1+r^2\omega^2} - u\rho a_1 - \dfrac{3\rho\omega^2 a_3 A_x^2}{4u} = 0 \end{cases} \tag{10}$$

Due to the complex form of the solution, it will not be cited.

The solution of the system (10) shows that in devices of this class – in contrast to linear ones (see eq. 7) – frequency of vibration depends on the flow velocity, therefore, depending on the selected set of system parameters, this can lead to four situations. There may exist one limit cycle, the frequency of which changes with the increase of the flow velocity and once reaches the value of the resonance frequency.

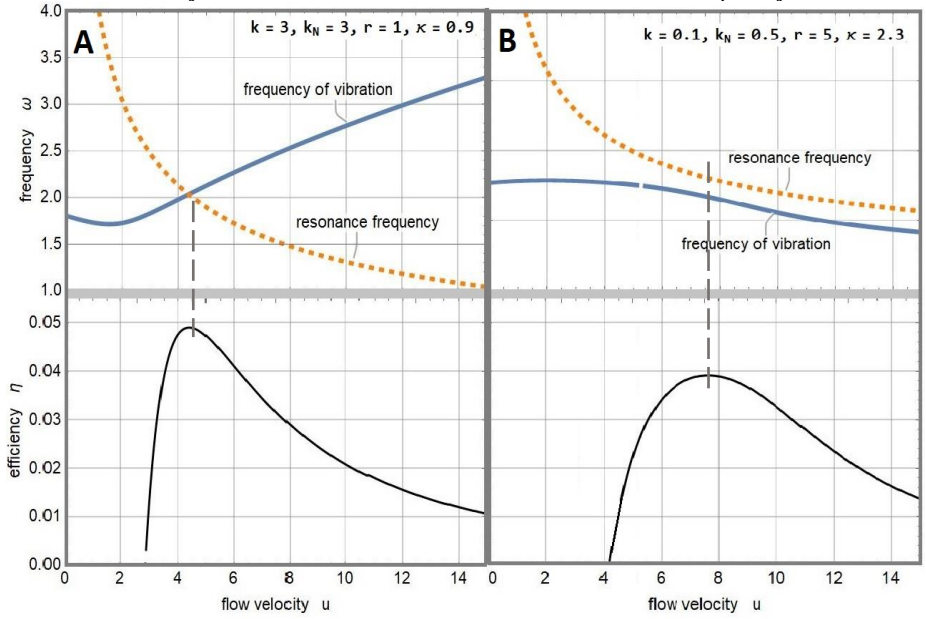

Figure 3. Efficiency vs flow velocity for different sets of parameters of nonlinear EH

This is a case devoid of advantages over a device with a linear characteristic – as shown in Figure 3A, as the flow velocity increases, the vibration frequency and the natural frequency of the system move away from each other faster than it would be for a constant vibration frequency, which leads to narrowing of the area resonance velocities. In the second, most unfavorable case, there is an absolutely non-resonance limit cycle, the occurrence of which leads to a significant decrease in efficiency (Fig. 3B). There may also be two limit cycles – high energy vibrations identical to the first case and nonresonant vibration (Fig. 4A).The last possibility is the occurrence of a limit cycle in which resonance occurs twice (Fig. 4B). This circumstance is most favorable from the point of view of the purpose of the work – a narrow spectrum of high efficiency can be extended by a second area of resonance overlapping it.

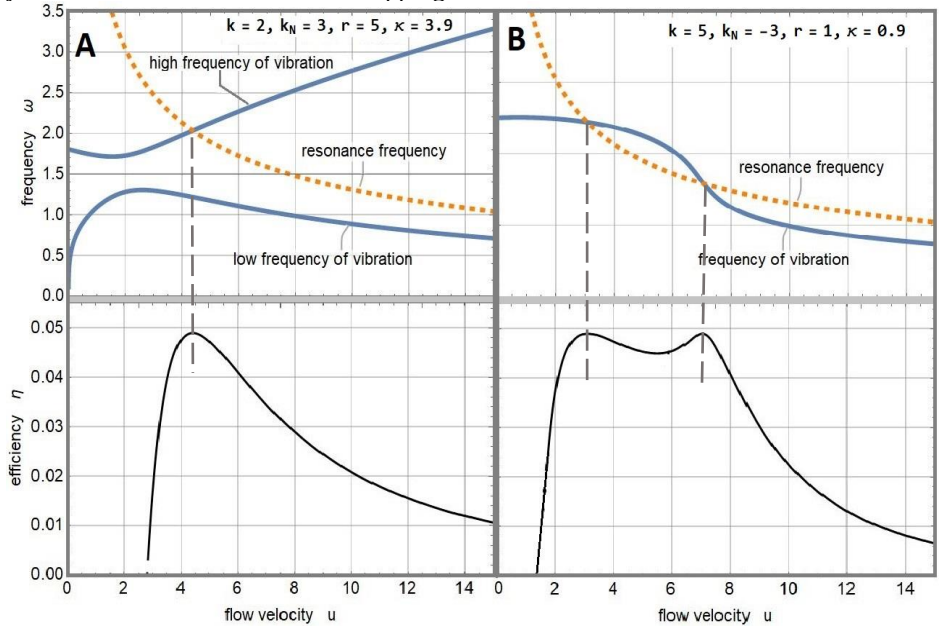

Figure 4. Efficiency vs flow velocity for different sets of parameters of nonlinear EH

It should be noted, that also in this case we observe the mechanism of narrowing of the first resonance area with decreasing critical velocity, which for its very low values results in a clear separation of both resonances with an area of low efficiency.

3. Delayed feedback control

The critical velocity of the energy harvester issue is inseparable from its stability – the system will be characterized by low critical velocity if it is easily destabilized. In turn, the ease of destabilization is a feature of systems with time delay [22], which has been frequently utilized to increase the efficiency of different types of energy harvesters [23] [24]. Therefore, we propose to replace the linear restoring force factor $k\,x(t)$ with a controlled actuator with a delay $k_d\,x(t-\tau)$ (delayed spring), where k_d

stands for controller gain and τ describes time delay, restoring force is then adopted as $S(x) = k_d\, x(t-\tau) + k_N\, x(t)^3$. The expected effect is to obtain the system with a low critical velocity whose areas of resonance operation are not separated by a low efficiency band. Usually, stability analysis is conducted by examining the sign of the real eigenvalues of the system - if even one of them is positive, the system is unstable. Studying the stability of systems with a delay is difficult due to the fact that the characteristic equation of models of this type is transcendent, so it has infinitely many solutions and thus it is not possible to analyze the signs of each of them. However, it is possible to examine the conditions for which at least one of the eigenvalues has a purely imaginary value, which is information about the occurrence of Hopf bifurcation. This procedure is outlined below. Characteristic equation of linearized model of the device takes the form:

$$\lambda^3 + \lambda^2\left(\frac{1}{r} - u\rho a_1\right) + \lambda\left(\kappa - \frac{u\rho a_1}{r} - k_d e^{-\lambda\tau}\right) - \frac{k_d e^{-\lambda\tau}}{r} = 0 \tag{11}$$

We are looking for conditions for which at least one of the eigenvalues has a purely imaginary value, therefore $\lambda = i\lambda_0$. After substituting this identity into eq. (11), expanding the exponential functions according to the Euler formula and separating the real and imaginary quantities we get the system of equations:

$$\begin{cases} -\dfrac{{\lambda_0}^2}{r} + {\lambda_0}^2 u\rho a_1 = \lambda_0\, k_d \sin(\lambda_0\tau) + \dfrac{k_d\cos(\lambda_0\tau)}{r} \\ -{\lambda_0}^3 - \dfrac{\lambda_0 u\rho a_1}{r} + \lambda_0\kappa = \lambda_0\, k_d\cos(\lambda_0\tau) - \dfrac{k_d\sin(\lambda_0\tau)}{r} \end{cases} \tag{12}$$

Adopting ${\lambda_0}^2 = \lambda_s$, and raising both equations to the square and then adding them by sides we get the equation from which the time delay τ has been eliminated:

$$\lambda_s^3 + \left(\frac{1}{r^2} - 2\kappa + (u\rho a_1)^2\right)\lambda_s^2 + \left(\kappa^2 - \frac{2u\kappa\rho a_1}{r} + \left(\frac{u\rho a_1}{r}\right)^2 - k_d^2\right)\lambda_s - \frac{k_d^2}{r^2} = 0 \tag{13}$$

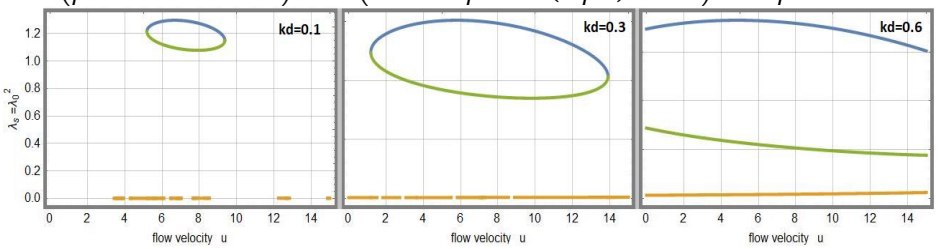

Figure 5. Values of roots $\lambda_s = {\lambda_0}^2$ vs flow velocity for $k_d = 0.1$, $k_d = 0.3$ and $k_d = 0.6$

Assumption about the existence of purely imaginary eigenvalues of the system will be met only for the set of parameters for which the above equation will have positive real roots in respect of λ_s. Assuming $\rho = 0.02$, $a_1 = 2.3$, $a_3 = -18$, $k_N = -1$, $r = 3$, $\kappa = 1.3$, below we present relationship of λ_s of flow velocity u for different controller gain k_d (Fig. 5).

Above graphs prove that the system can be unstable even for the flow velocity u = 0 and remain unstable for faster flows, if gain k_d is properly selected. It is also necessary to specify the τ delay limits, which for calculated $\lambda_s \in \mathbb{R}^+$ will cause instability. Solving the system of equations eq. 12 for $\tau > 0$ leads to the following identity:

$$\tau = \frac{1}{\lambda_0}\left(\text{arctg}\left(\frac{r\kappa - u(1+r^2{\lambda_0}^2)\rho a_1}{\lambda_0 - r^2\kappa\lambda_0 + r^2{\lambda_0}^3} + 2k\pi\right)\right), k = 0,1,2,\ldots \tag{14}$$

The delayed feedback controller will effectively destabilize the system if its parameters are selected in accordance with the above procedure. However, it should be cautioned that the controller will be powered by an external source of energy, therefore, to correctly assess the impact of delayed feedback on the device efficiency, it is necessary to determine the average power P_c consumed by the controller. Assuming the previously adopted form of solutions (eq. 5-6) and $x(t-\tau) = A_x \cos(t-\tau)$, it can be defined as:

$$P_c = \frac{1}{T}\int_0^T k_d\, x(t-\tau)\, \dot{x}(t)\, dt = \frac{1}{2}k_d \omega {A_x}^2 \sin(\tau\omega) \tag{15}$$

The unknown values of A_x and ω can be determined by solving the system of equations obtained by applying the harmonic balance method, while expanding the appearing $\sin(\tau\omega)$ and $\cos(\tau\omega)$ elements in the Maclaurin series in term of ω to at least third order:

$$\begin{cases} \omega^2 - k_d + \frac{1}{2}k_d\tau^2\omega^2 - \frac{r^2\kappa\omega^2}{1+r^2\omega^2} - \frac{3k_N A_x^2}{4} = 0 \\ \frac{1}{6}k_d\tau^3\omega^3 - k_d\tau\omega + \frac{r\kappa\omega}{1+r^2\omega^2} - u\rho\omega a_1 - \frac{3\rho\omega^3 a_3 A_x^2}{4u} = 0 \end{cases} \tag{16}$$

The efficiency of the controlled system is therefore given by the expression:

$$\eta = \frac{P - P_c}{P_t} = \frac{A_x^2\,\omega(r\kappa\omega - k_d(1+r^2\omega^2)\sin(\tau\omega))}{2\rho u^3(1+r^2\omega^2)} \tag{17}$$

4. Results and conclusions

Figure 6 shows graphs of the dependence of efficiency on the flow velocity for different energy harvester variants with the same, very low, critical velocities. On the first of them, concerning the device with delayed feedback control (Fig. 6-1), two resonance peaks can be recognized, and they occurred for velocities respectively: $u = 0.32$ and $u = 1.61$. By application the controller, both resonances can be close enough to create one, relatively wide band of high efficiency. In spectrum from $u = 0.18$ up to $u = 2.16$ the efficiency does not decrease more than by 5%. In the case of an uncontrolled device with two resonances (Fig. 6-2), this effect is not possible due to the fact that the distance between resonances is inversely proportional to the critical velocity. This leads to an unfavorable situation in which the resonance areas are separated by a low efficiency band. High efficiency spectrum occurs only in the narrow velocity band from $u = 0.18$ to $u = 0.54$, therefore it is 5.5 times narrower than for controlled EH. As shown on figure 6-2, for the higher velocities, next high efficiency band is again present, but it should be emphasized that for such low critical velocities, the occurrence of a second resonance is conditioned by the supercritical Hopf bifurcation, which is associated with setting up an appropriate initial conditions, and this may not be possible during the operation of the device. Figure 6-3 applies to a single-resonance nonlinear device and its presented to emphasize its low utility in contrast to other variants. Considering the above facts, it can be concluded

that the utility of noncontrolled devices with low critical velocities is poor and they are significantly inferior to energy harvesters with delayed feedback control.

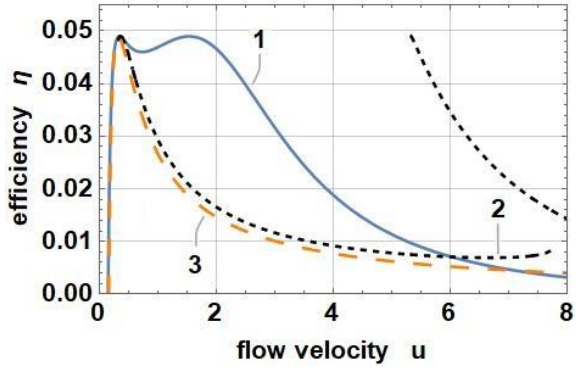

Figure 6. Efficiency vs flow velocity for different variants of device

Acknowledgments

This paper was financially supported by the grant: 0612/SBAD/3558

References

1. J.P. Den Hartog, *Mechanical Vibrations*, fourth ed. McGraw-Hill, New York, USA (1956).
2. M. Novak, *Aeroelastic galloping of prismatic bodies*, Journal of the Engineering Mechanics Division, 96 (1969) 115–142.
3. Y. Ng, S. C. Luo, Y. T. Chew, *On using high-order polynomial curve fits in the quasi-steady theory for square-cylinder galloping*, J. Fluid and Structures, 20-1 (2005). 141–146.
4. A. Barrero-Gil, G. Alonso, and A. Sanz-Andrés, *Energy harvesting from transverse galloping*, Journal of Sound and Vibration, 329(14) (2010) 2873– 2883.
5. S. Boisseau, G. Despesse, B. Ahmed Seddik, *Electrostatic Energy Harvesting Systems*, Small-Scale Energy Harvesting, Intech (2012)
6. A. Kumar, S. S. Balpande, S. C. Anjankar, *Electromagnetic Energy Harvester for Low Frequency Vibrations Using MEMS*, Procedia Computer Science 79 (2016) 785-792.
7. H. L. Dai, A. Abdelkefi, U. Javed, L. Wang, *Modeling and performance of electromagnetic energy harvesting from galloping oscillations*, Smart Materials and Structures, 24(4) (2015).
8. A. Haroun, I. Yamada, S. Warisawa, *Investigation of Kinetic Energy Harvesting from Human Body Motion Activities using Free/Impact Based Micro Electromagnetic Generator*, Jourunal of Diabetes and Cholesterol Metabolism, 1 (2016) 12-16.
9. A. Abdelkefi, A. Nayfeh, M. R. Hajj, *Enhancement of power harvesting from piezoaeroelastic systems*, Nonlinear Dynamics, 68(4) (2016).

10. A. Abdelkefi, A. Nayfeh, M. R. Hajj, *Modeling and analysis of piezoaeroelastic energy harvesters*, Nonlinear Dynamics, 67(2) (2011) 925-939.
11. S. Priya, D. J. Inman, Energy Harvesting Technologies, Springer, New York, USA (2009)
12. C. Howells, *Piezoelectric energy harvesting*, Energy Conversion and Management, 50 (2009) 1847-1850.
13. C. De Marqui, A. Erturk, D. J. Inman, *An electromechanical finite element model for piezoelectric energy harvester plates*, Journal of Sound and Vibration 327 (2019) 9-25.
14. G. Alonso, J. Meseguer, A. Sanz-Andres, E. Valero, *On the galloping instability of two-dimensional bodies having elliptical cross-sections*, Journal of Wind Engineering and Industrial Aerodynamics, 98 (2010) 438-448.
15. N. J. Nikitas, H. G. Macdonald, *Misconceptions and Generalizations of the Den Hartog Galloping Criterion*, Journal of Engineering Mechanics, 140 (2014).
16. J. Meseguer, A. Sanz-Andres, G. Alonso, *Determination of Maximum Mechanical Energy Efficiency in Energy Galloping Systems*, Journal of Engineering Mechanics, 141 (2015) 1355–1363.
17. A. Abdelkefi, M. R. Hajj, A. Nayfeh, *Power harvesting from transverse galloping of square cylinder*, Nonlinear Dynamics, 70 (2012).
18. S. Jayant, M. Rohan, *Harvesting wind energy using a galloping piezoelectric beam*, Journal of Vibration and Acoustics, 134(1) (2012)
19. Y. Wu, D. Li, J. Xiang, *Dimensionless modeling and nonlinear analysis of a coupled pitch–plunge–leadlag airfoil-based piezoaeroelastic energy harvesting system*, Nonlinear Dynamics, 92(2) (2018) 153–167.
20. R. Vasconcellos, A. Abdelkefi, *Nonlinear dynamical analysis of an aeroelastic system with multi-segmented moment in the pitch degree-of-freedom*, Communications in Nonlinear Science and Numerical Simulation, 20(1) (2015) 324-334.
21. Y. Wu, D. Li, J. Xiang, A. Da Ronch, *A modified airfoil-based piezoaeroelastic energy harvester with double plunge degrees of freedom*, Theoretical and Applied Mechanics Letters, 6 (2016) 244-247.
22. K. Gu, V. L. Kharitonov, J. Chen, *Stability of time delay systems*, Birkhäuser, Boston (2003).
23. A. S. Kammer, N. Olgac, *Delayed feedback control scheme for improved energy harvesting using piezoelectric networks*, Journal of Intelligent Material Systems and Structures, 29(8) (2018) 1546–1559.
24. B. Amine, I. Kirrou, M. Belhaq, *Energy harvesting of nonlinear damping system under time delayed feedback gain*, MATEC Web of Conferences, 83 (2016).